Polymer 50 (2009) 357–365

Contents lists available at ScienceDirect

Polymer

journal homepage: www.elsevier.com/locate/polymer

Particle formation and growth in *ab initio* emulsifier-free emulsion polymerisation under monomer-starved conditions

Yan Chen, Shahriar Sajjadi*

Division of Engineering, ECLAT, King's College London, London WC2R 2LS, UK

ARTICLE INFO

Article history:
Received 26 June 2008
Received in revised form
30 October 2008
Accepted 6 November 2008
Available online 20 November 2008

Keywords:
Particle formation
Particle coagulation
Emulsifier-free emulsion polymerisation

ABSTRACT

Particle formation and growth in the monomer-starved emulsifier-free emulsion polymerisation of monomers with different water solubility including methyl acrylate (MA), methyl methacrylate (MMA), and vinyl acetate (VA) were studied. The rate of formation of precursor particles, via homogenous nucleation, is proportional to the monomer concentration in the water phase. One may think that the maximum number of particles will be obtained when the water phase is saturated with the monomer. The number of PMA particles showed a maximum when the water phase was starved with the monomer. The number of PVA particles did not show any sensitivity to the monomer concentration in the water phase. More unexpectedly the final number of PMMA particles showed a minimum when the water phase was just saturated with the monomer. The minimum in the final number of PMMA particles was correlated with the enhanced rate of particle growth due to the gel effect. Under monomer-starved conditions, the number of particles produced was in the order of water solubility of the monomers; MA > VA > MMA. A reverse order was produced under monomer-saturated conditions as particle coagulation became progressively more important for some of the monomers.

1. Introduction

Emulsion polymerisation is an important industrial process for manufacturing of wide varieties of polymer latexes. Emulsifier-free emulsion polymerisation is of both industrial and academic interest since the resulting polymer latex is free from absorbed surfactant and could contain highly monodisperse polymer particles [1,2]. For emulsifier-free emulsion polymerisation, Fitch proposed a mechanism of homogenous nucleation, whereby radicals would propagate in the water phase by free radical polymerisation mechanism [3]. Oligomeric radicals continue to grow by propagation until they reach a critical size at which they become surface active – *i.e.* a surfactant. At this critical size, they may have a number of fates. If they terminate in the aqueous phase, they will act as an *in situ* surfactant. They may also enter either an existing polymer particle or may continue to propagate. After further propagation in the water phase the polymer chain reaches a critical size, j_{cr}, at which it precipitates as a precursor particle. Precursor particles are only marginally stable since small particles have a large amount of free energy across their surface. Precursor particles grow by two mechanisms: propagation, or coagulation with other precursor particles [4,5]. By either way, precursor particles continue to expand until they are sufficiently stable.

The monomer concentration in the water phase can probably be considered as the most influential parameter in the kinetics of emulsifier-free emulsion polymerisations. This is because the rate of formation of precursor particles is directly related to the monomer concentration in the water phase. The kinetics of emulsifier-free emulsion polymerisation has been studied in great detail. A few investigators have considered the effect of monomer concentration on the kinetics of polymerisation as well as particle size [6–8]. However, these studies either concentrated on a certain range of monomer concentration or did not elaborate on the kinetic features in the region of transition from monomer-starved to monomer-saturated conditions. One application of monomer-starved polymerisation is usually encountered in semibatch processes. Emulsifier-free semibatch emulsion polymerisation processes are designed for preparing monodisperse and structured particles with good stability [9]. Semibatch processes are usually started with a small quantity of monomer charge to produce seed particles followed by addition of monomer to grow the particles [10]. Therefore, it is quite important to understand the kinetics of monomer-starved emulsifier-free emulsion polymerisation and the conditions under which particles with desired size can be produced.

The purpose of this article is twofold; first is to study particle formation and growth in *ab initio* emulsifier-free emulsion polymerisation in a wide range of monomer concentrations and in

* Corresponding author. Tel.: +44 020 7848 2322; fax: +44 020 7848 2932.
E-mail address: shahriar.sajjadi-emami@kcl.ac.uk (S. Sajjadi).

0032-3861/$ – see front matter © 2008 Elsevier Ltd. All rights reserved.
doi:10.1016/j.polymer.2008.11.013

particular in the monomer-starved range. Second, to show how the pattern of particle formation versus monomer concentration may change with monomer type and solubility in water.

2. Experimental

2.1. Chemicals

Analytical grade potassium persulfate (Aldrich) and sodium hydrogen carbonate (Aldrich) were used as initiator and buffer, respectively. The monomers methyl acrylate (MA), vinyl acetate (VA), and methyl methacrylate (MMA) were supplied at 99.9% purity by Aldrich, inhibited against thermal polymerisation with trace quantities of an inhibitor. This inhibitor was removed prior to the use by an ion exchange column (Aldrich). Uninhibited monomers were stored at −20 °C and used within a week.

2.2. Apparatus

The apparatus consists of a round-bottomed jacketed glass reaction vessel of 1 l internal capacity. The reactor was equipped with a four-bladed stainless steel flat turbine type impeller with a width of 1/2 of vessel diameter and standard four baffle plates with the width of 1/10 of vessel diameter located at 90° intervals. The stirrer rate was kept constant at 300 rpm for most reactions. The temperature of the reactor contents was controlled at 60 ± 1.0 °C by pumping water with appropriate temperature from a water bath through the jacket. Sampling was carried out at the desired time interval by removing an aliquot of 1–2 g latex by a hypodermic syringe through a septum.

2.3. Procedure

The reactor was initially charged with most of the de-ionised water (580 ml) and the buffer (0.0503 g or 1×10^{-3} mol/l) and allowed to heat up to the desired reaction temperature while being purged with nitrogen under strong mixing (550 rpm). The purging continued at the reaction temperature for another 15 min. Then the nitrogen line was lifted to sit well above the surface of the water to prevent evaporation of monomer from the reaction mixture and also to allow for degassing of the water. The nitrogen rate was reduced to provide only slight overpressure and the agitation speed was then reduced to 300 rpm. A weighed quantity of a monomer, defined as a percentage of its saturation concentration (solubility) in water, was added into the water. The system was allowed to return to reaction temperature. The initiator solution (0.1622 g or 1×10^{-3} mol/l), dissolved in 20 ml of de-ionised water from the overall recipe, was then added to the vessel. An inhibition period in the order of 3.0–9.0 min was observed for polymerisation reactions to start, depending on the monomer type and concentration. The onset of reaction was continuously monitored by sampling from the vessel and precipitating the samples in methanol. The reaction time *zero* for the start of reaction was considered when polymer was detected in the reaction mixture.

In order to be able to compare different monomers in terms of their water solubility, we present the results in terms of percentage or ratio of the saturation concentration of the monomers in water; saturation ratio (S_r). The saturation ratio of $S_r = 100\%$ can be defined as the concentration at which water is saturated with monomer and no more monomer will dissolve in water. At $S_r < 100\%$, the monomer will dissolve completely into the water which is starved with monomer. At $S_r > 100\%$ the excess monomer will separate out into monomer droplet phase. The saturation concentration of monomers MA, VA, and MMA in water is 5.0, 2.5, and 1.5 wt%, respectively. These correspond to 0.58, 0.29, and 0.15 mol/l for the above monomers, respectively.

2.4. Measurements

Conversions were measured gravimetrically. The initial rate of polymerisation reaction (R_p) was calculated from the gradient of the initial linear part of polymer mass–time curves for each experiment. The *z*-average diameter of particles ($D_{z,ds}$) was measured using laser light scattering (nanosizer, Malvern).

Given the mass of polymer in the system and the average particle diameter, it is possible to calculate the number of particles (per unit volume of the aqueous phase; $l^{-1}_{(aq)}$) according to the following equation:

$$N_p = 6m_p/\pi D_v^3 \rho_p \quad (1)$$

The numerator, m_p, gives the mass of polymer (per unit volume of the aqueous phase; g l^{-1}) in the system at any given time, D_v is the average-volume diameter of unswollen polymer particles, and ρ_p is the polymer density which is 1.22, 1.16, 1.178 g/ml for PMA, PVA, and PMMA, respectively [11].

For calculation of N_p, as given in Eq. (1), volume-average diameter should be known. It is known that dynamic laser light scattering gives an estimation of hydrodynamic diameter of particles, and also produces *z*-average diameter which is larger than the volume average. The application of *z*-average hydrodynamic diameter to the above equation causes an underestimation of N_p. In order to obtain a better estimation of volume-average diameter, some final samples were examined by using transmission electron microscopy (TEM; Nippon Denshi Co., Japan, 200 kV) and analysed for size distributions. TEM provides the complete distribution data from which all average diameters can be calculated. To construct PSD curves, at least 1000 particles were measured. The number-, weight-, volume-, and *z*-average particle diameters (D_n, D_v, D_w, and D_z, respectively) and polydispersity index (PDI) were calculated using the following equations:

$$D_n = \sum n_i D_i / \sum n_i \quad (2)$$

$$D_w = \sum n_i D_i^4 / \sum n_i D_i^3 \quad (3)$$

$$D_v = \left[\sum n_i D_i^3 / \sum n_i \right]^{1/3} \quad (4)$$

$$D_z = \left[\sum n_i D_i^8 / \sum n_i D_i^6 \right]^{1/2} \quad (5)$$

$$\mathrm{PDI} = D_w / D_n \quad (6)$$

All samples examined had a rather sharp and monomodal distribution, which is a characteristic feature of emulsifier-free emulsion polymerisation, as shown in Fig. 1. The PDI of the final latexes was found to be 1.02 ± 0.008. The ratio of D_v/D_z of latexes, obtained by TEM, was 0.98 ± 0.01. From the comparison of *z*-average diameter (D_z) obtained by TEM (using Eq. (5)) with *z*-average hydrodynamic diameter directly obtained by laser light scattering ($D_{z,ds}$), and relating their ratio to D_v (using Eq. (4)), the conversion factor of $C_f = 0.84 \pm 0.01$ was found so that $D_v = C_f \times D_{z,ds}$.

Most experiments were carried out twice. The reproducibility of the results was quite good as there was no significant change in the rate of polymerisation and particle size. Only minor variations in the final conversions were recorded for some reproduced runs.

3. Results

3.1. Mass of polymer versus time

Figs. 2–4 show the variations in the mass of polymer produced versus time for MA, VA, and MMA monomers, respectively. It is

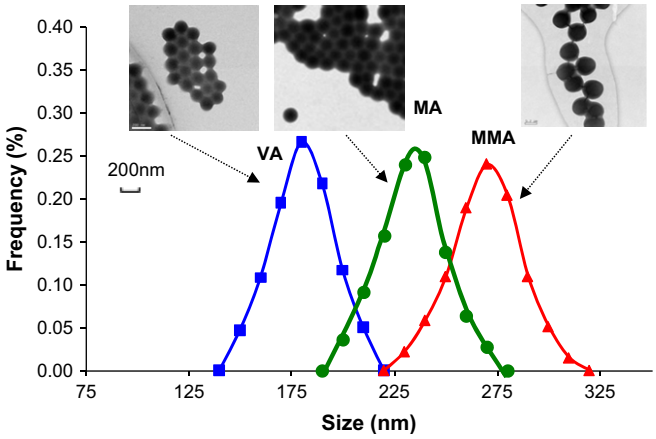

Fig. 1. Final particle size distribution obtained by TEM for MA, VA, and MMA monomers at S_r values of 100%, 100% and 75%, respectively (the insets show the corresponding TEM micrographs).

obvious from the plots that the initial rate of polymerisation (R_p; mol/l(aq) s or g/l(aq) min) increases with the monomer concentration for all monomers for $S_r \leq 100\%$. The exponent for the initial rate of polymerisation in terms of monomer concentration in the water phase, $R_p = [M]_w^a$, was found to be 1.71, 1.32, and 1.24 for MA, VA, and MMA monomers, respectively (the exponent for VA only corresponds to a limited range of $S_r = 25$–50% as R_p approached almost a constant value for the higher range of S_r).

For $S_r > 100\%$, different trends were observed for the monomers. For the most water-soluble monomer studied, MA, the rate of polymerisation slightly increased with the monomer concentration. For VA monomer, the initial rate of polymerisation did not vary significantly with the monomer concentration, though some variations in the rate occurred later during the polymerisation. One

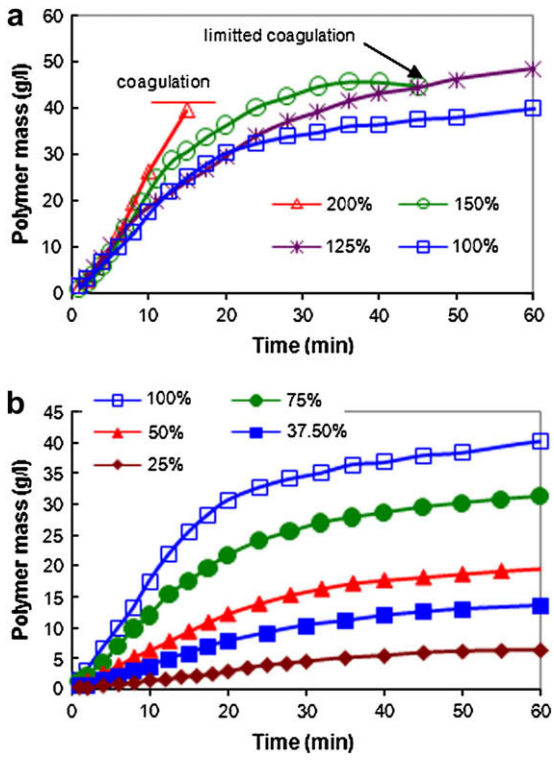

Fig. 2. Mass of PMA versus time for monomer saturation ratios of (a) $S_r \geq 100\%$ and (b) $S_r \leq 100\%$.

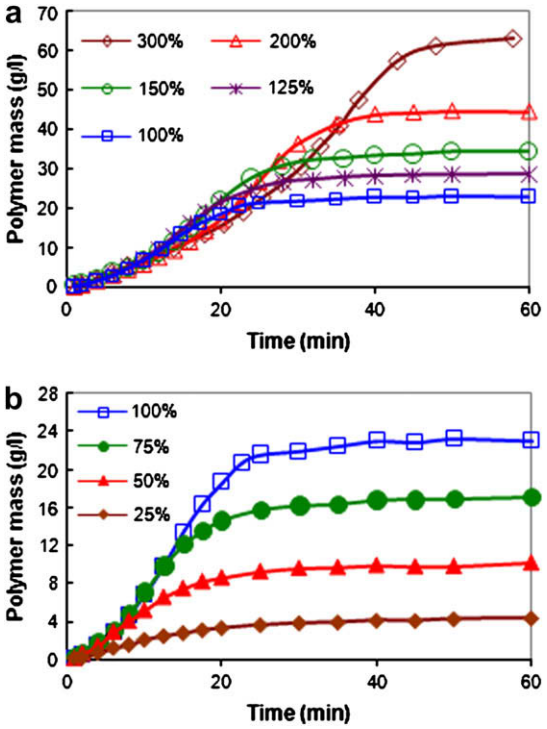

Fig. 3. Mass of PVA versus time for monomer saturation ratios of (a) $S_r \geq 100\%$ and (b) $S_r \leq 100\%$.

of the features of VA emulsion polymerisation is that R_p is independent of monomer concentration in the particles up to high conversions. For MMA monomer, the least water-soluble monomer used, R_p surprisingly decreased with increasing monomer concentration. At a later stage of reaction, however, the rate of polymerisation underwent massive auto-acceleration due to the gel effect [12].

The final conversion increased with monomer concentration for all monomers (not shown). Since these monomers are partially water soluble, there will be a certain amount of monomer that will remain dissolved in the water and not be easily available for reaction. The lower was the monomer concentration, the larger fraction of monomer remained in the water phase and the smaller was the final conversion.

3.2. Size of particles

The results for particle size versus time are shown in Figs. 5–7 for the monomers. The size of final particles increased with monomer concentration, as was expected. The size of particles at the outset of polymerisation increased with monomer concentration for $S_r \leq 100\%$. The effect, however, was less obvious for VA monomer. The results suggest that the monomer concentration in the water phase can significantly affect the kinetics of particle formation and growth.

For $S_r \geq 100\%$, where monomer droplets exist, the size of particles at the outset of polymerisation varied slightly with concentration of MA and MMA monomers. However, it became progressively different with reaction time for both monomers. The size of particles for VA monomer was similar in the course of reaction until high conversions. A constant pattern of particle size–reaction time in the region of $S_r \geq 100\%$ corroborates with a constant rate of polymerisation in the same region for VA monomer (see Figs. 3a and 6a) [13,14]. For MA monomer with $S_r = 200\%$, polymerisation had to be stopped at an intermediate

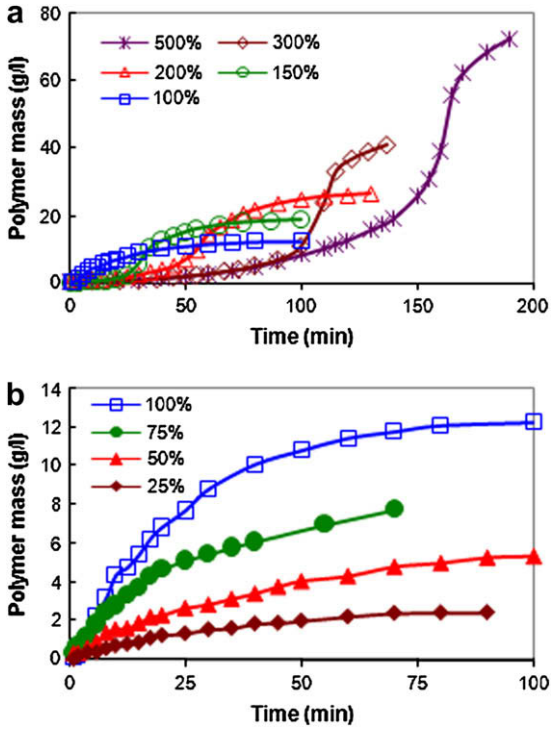

Fig. 4. Mass of PMMA versus time for monomer saturation ratios of (a) $S_r \geq 100\%$ and (b) $S_r \leq 100\%$.

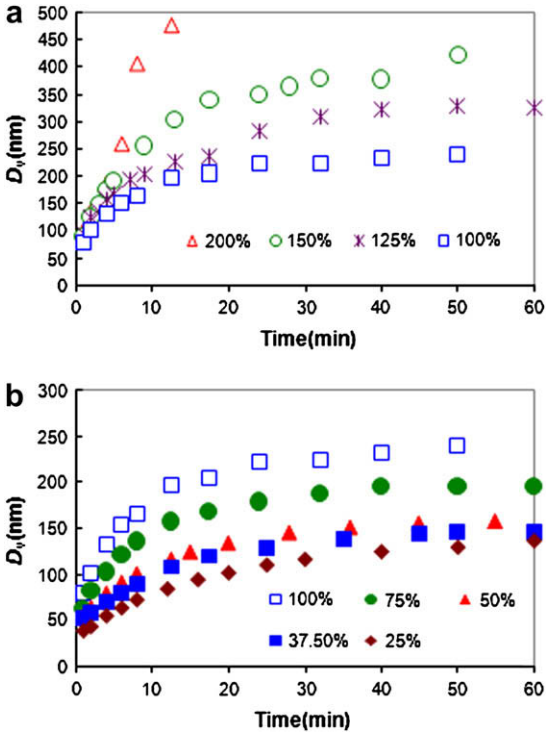

Fig. 5. D_v versus time for MA polymerisation for monomer saturation ratios of (a) $S_r \geq 100\%$ and (b) $S_r \leq 100\%$.

conversion due to a massive coagulation. Limited coagulation also occurred in the later stage of MA polymerisation with $S_r = 150\%$. These suggest that particle coagulation contributes to particle growth for this monomer.

In opposite to MA polymerisation, the size of particles in MMA polymerisation decreased with increasing monomer concentration for $S_r > 100\%$. One may consider the formation of small particles, as shown in Fig. 7a, as the cause for a low rate of polymerisation in this region. Zimmt [15] showed that any increase in the rate of polymerisation of MMA because of diffusion-controlled termination (gel effect) can only be observed for particles with swollen diameter of 65 nm and larger. The minimum size of the unswollen particles formed in the initial stage of polymerisations was 50 nm (>65 nm in terms of monomer-swollen diameter) indicating that the particles were potentially capable of undergoing the gel effect. This refutes the size of particles as the main cause for a sharp drop in the rate of polymerisation. We will show in the next section that the reduced growth of particles is in fact a consequence of low rate of polymerisation and not the cause for it.

4. Discussion

4.1. Rate of polymerisation

In the region of $S_r > 100\%$, the initial rate of polymerisation slightly increased with monomer concentration for MA, remained almost constant for VA, and slightly decreased for MMA. In the region of $S_r \leq 100\%$, the rate of polymerisation increased with monomer concentration for all three monomers. One important observation for MMA monomer was that the rate of polymerisation was greater under monomer-starved condition than under monomer-saturated one, as seen in Fig. 4. This is quite intriguing and deserves further explanation. It is clear from Fig. 4 that R_p for the run with $S_r = 25\%$ is even greater than that with $S_r = 500\%$. This behaviour has been previously observed for MMA emulsifier-free emulsion polymerisation [7,8], however, has not been explained yet. The reason that the rate of polymerisation of MMA in the region of $S_r < 100\%$ increased, in comparison to that in the region of $S_r > 100\%$, can be attributed to the gel effect, which occurs in particles containing a high polymer weight ratio (w_p).

The following empirical equation was used to correlate the monomer concentration in the water phase ($[M]_w$) to that in the polymer phase ($[M]_p$) [16].

$$\frac{[M]_w}{[M]_{w,sat}} = \left(\frac{[M]_p}{[M]_{p,sat}}\right)^{0.60} \tag{7}$$

where $[M]_{p,sat}$ and $[M]_{w,sat}$ are the corresponding saturation values. The amount of free monomer in the polymer phase is:

$$m_p = m_0 - \left([M]_w V_w + [M]_p V_p + [M]_d V_d\right) M_{mon} \tag{8}$$

where m_0 indicates the initial amount of monomer in the vessel, m_p is the weight of polymer in the particles, M_{mon} is the molecular weight of the monomer, and V_w, V_p, and V_d are the volume of water phase, polymer phase, and monomer droplet phase per unit volume of water phase, respectively. The polymer weight fraction in polymer particle (w_p) is

$$w_p = m_p/(m_p + m_m) \quad \text{for } w_p \geq w_{p,sat} = 0.33 \tag{9}$$

where $w_{p,sat} = 0.33$ is the conversion above which polymerisation shifts from monomer-saturated condition to monomer-starved condition, and m_m ($=[M]_p V_p M_{mon}$) is the weight of monomer in polymer particles. w_p is correlated with $[M]_p$ according to the following equation:

$$[M]_p = \frac{1 - w_p}{\left(\frac{1 - w_p}{\rho_m} + \frac{w_p}{\rho_p}\right) M_{mon}} \tag{10}$$

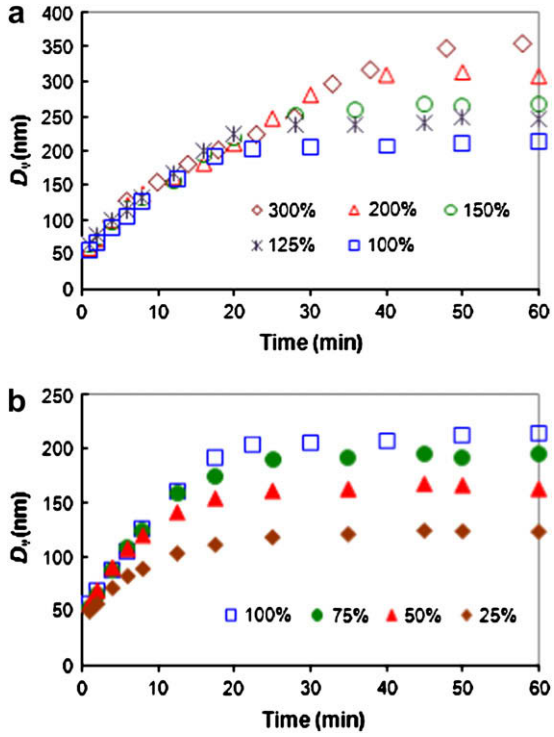

Fig. 6. D_v versus time for VA polymerisation for monomer saturation ratios of (a) $S_r \geq 100\%$ and (b) $S_r \leq 100\%$.

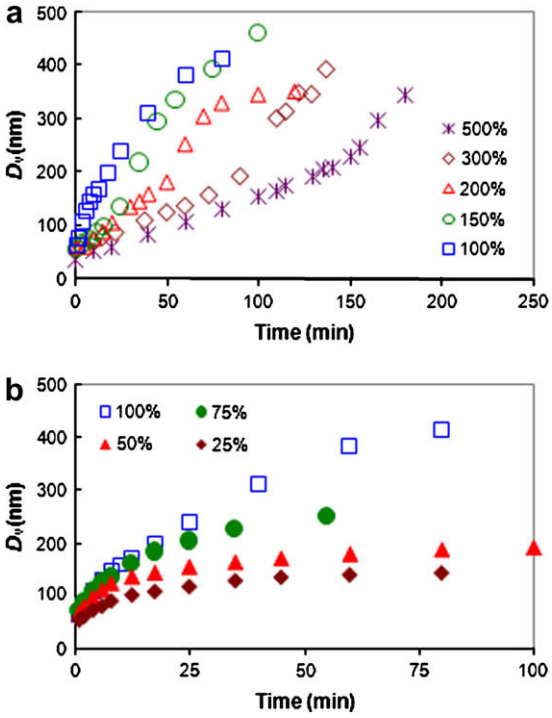

Fig. 7. D_v versus time for MMA polymerisation for monomer saturation ratios of (a) $S_r \geq 100\%$ and (b) $S_r \leq 100\%$.

where ρ_m is the density of the monomer. Assuming $[M]_{p,sat}$ and $[M]_{w,sat}$ to be 6.60 mol/l and 0.15 mol/l [11], respectively, and knowing m_p from the rate data, w_p can be calculated using Eqs. (7)–(10).

Fig. 8 shows the variations in the calculated w_p with reaction time for MMA monomer. It is assumed that particles are saturated with the monomer ($w_p = w_{p,sat} = 0.33$) in the early stage of polymerisation if $w_p \leq w_{p,sat}$. Note that for $S_r \leq 100\%$, particles are monomer starved right from the beginning.

Conventional MMA emulsion polymerisation in interval III, or at high conversions, is usually treated as pseudo-bulk kinetics where the gel effect is predominant. Particles under such conditions can contain more than one growing radical because of an increase in the viscosity of particles and termination reaction being controlled by diffusion. As a result, the rate of polymerisation increases significantly. In pseudo-bulk kinetics the rate of polymerisation is independent of N_p, as this can be easily inferred from the slope of the reaction rates in the region of the gel effect (see Figs. 4 and 8).

It should be noted that the increase in the rate of polymerisation under starved conditions may not be operative for the conventional MMA emulsion polymerisation. No significant change in R_p with monomer concentration can be inferred from the data reported by Nomura and Fujita [17] on *ab initio* MMA emulsion polymerisation in the presence of a surfactant. This is probably due to the fact that particles formed in the presence of surfactant were quite small and could not undergo the gel effect [15], as explained before.

Table 1 shows the average radical number per particle, $\bar{n}$, in the initial stage of MMA polymerisations carried out using different monomer concentrations. $\bar{n}$ was calculated using the following equation:

$$\bar{n} = \frac{R_p N_A}{k_p [M]_p N_p} \tag{11}$$

The values of $\bar{n}$ reveal a significant decrease with increasing S_r. The large values of $\bar{n}$ for $S_r \leq 100\%$ represent polymerisations at the high conversion (gel effect) during which particles could accumulate a large number of radicals due to the reduced rate of termination. For the runs with $S_r \gg 100\%$, small values of $\bar{n}$ were obtained. Particles in this region are most probably confined to a zero–one system. In a zero–one system, secondary radical entry into a particle already containing a growing radical leads to instantaneous termination. At very low values of $\bar{n}$, the fate of a growing radical in particles is termination by chain transfer to monomer followed by desorption of the monomeric radical into the aqueous phase [18]. It can be concluded that with increasing monomer concentration, the kinetic regime of polymerisation shifts from a pseudo-bulk kinetics to a zero–one system.

4.2. Diffusion-controlled monomer transport

The presence of a large number of monomer droplets in the reaction mixture allows for a rapid diffusion of monomer into polymer particles via the water phase. The diffusion-controlled monomer transport is more likely to be operative at low monomer concentrations where the total surface area of monomer droplets is small. A slight increase in the rate of MA polymerisation with S_r in

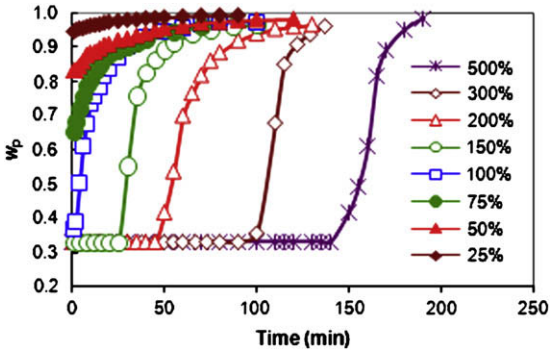

Fig. 8. w_p versus time for MMA polymerisation with different saturation concentration ratios (S_r).

Table 1
Calculated $\bar{n}$ for MMA emulsion polymerisation with different monomer saturation ratios.

S_r (%)	25	50	75	100	150	200	300	500
$[M]_p$[a] (mol/l)	0.54	1.79	3.06	4.36	6.58	6.58	6.58	6.58
N_p[b] ($\times 10^{-15}$ 1/l)	1.15	1.25	1.64	1.51	1.11	1.51	1.64	2.29
R_p ($\times 10^5$ mol/l s)	1.21	2.51	5.15	6.32	0.87	0.82	0.50	0.39
$\bar{n}$[c]	13.96	8.16	7.47	6.95	0.86	0.60	0.33	0.19

[a] An average $[M]_p$ corresponding to the linear part of the reaction rate–time curve has been considered.
[b] An average N_p corresponding to the linear part of the reaction rate–time curve has been considered.
[c] $\bar{n}$ is calculated using Eq. (11). The propagation rate constant, $k_p = 830$ l/mol s, was obtained from the interpolation of the data given in Ref. [11].

the region of $S_r = 100$–200% suggests a possible limitation in monomer transport. Indications of limitation in MMA monomer transport can be inferred from the data given in Table 1. For the intermediate range of S_r, 100–200%, where monomer droplets exist and particles are theoretically saturated with the monomer, $\bar{n}$ has a value within the lower range of pseudo-bulk model. We think that particles are monomer starved in this region so that w_p in the particles is above the saturation value ($w_p > w_{p,sat}$) even though there exists monomer droplets. The argument is supported by the particle size data, as shown in Fig. 7a. Particles formed early in the reaction became smaller with increasing S_r (in the region of $S_r >$ 100%), probably, as a result of a high rate of radical termination in the particles (small $\bar{n}$). There is another sign of diffusion-controlled limitation within the particles which can be inferred from the onset of the gel effect, as shown in Fig. 4a. The slope of polymer mass–time data starts to increase at an earlier conversion than that shown in Fig. 8 based on the assumption of equilibrium distribution of the monomer ($w_p = 0.33$). For VA monomer in the region of $S_r > 100\%$, the initial rate of polymerisation was independent of monomer concentration. Consequently, it is not possible to discuss the limitation in VA monomer transport by analysing the reaction rate data.

In order to provide an evidence for diffusion-controlled monomer transport occurring in the systems under study, experiments were carried out using a higher stirring speed than the previous experiments; 325 rpm. A high rate of agitation serves to expand the interfacial area by making small droplets and thus may improve the rate of monomer transport. The rate of MA and MMA polymerisations and the number of resulting particles are shown in Fig. 9. It can be observed that R_p increased with rpm for MA but decreased for MMA. These trends, though seemingly opposite, reflect a limitation in monomer transport for both monomers.

The diffusion-controlled monomer transport from the droplets to the growing polymer particles is operative for MA monomer due to its rapid rate of polymerisation. For this monomer, R_p increased with rpm, similar to the effect produced by increasing S_r. Note that the increase in R_p occurred despite the concomitant reduction in the number of particles due to particle coagulation, as shown in the insets of Fig. 9a. Assuming that conventional Weber number correlations apply to the monomer drops in the current system (d_{32} α rpm$^{-0.75}$ to rpm$^{-1.2}$ for coalescence and break up dependent regimes, respectively, d_{32} is the average surface diameter), then an increase of stirrer speed from 300 rpm to 325 rpm would decrease the drop size by about 9%, and increase the total surface area of drops by almost the same value (the surface area of drops per unit volume of the dispersed phase is inversely proportional to the size of drops). This is consistent with the increase in the rate of MA polymerisation with rpm, which was around 12% (note that the mass transfer coefficient also increases with rpm). Knowing R_p and N_p, from the insets of Fig. 9b, it is possible to calculate $[M]_p\bar{n}$ from Eq. (11). Assuming a constant N_p for the early stage of polymerisation at both rpm values, the value of $[M]_p\bar{n}$ shows a 12% rise with the increase in rpm. PMA is a soft polymer that does not allow diffusion-controlled termination to occur. Therefore, the increase in $[M]_p\bar{n}$ may be attributed to a higher $[M]_p$. This confirms that an increase in rpm will enhance monomer transport.

For MMA monomer, the increase in rpm produced a lower rate of polymerisation, similar to the effects produced by increasing S_r, but almost with the same number of initial particles. The calculations show that an increase from 300 to 325 rpm reduced $[M]_p\bar{n}$ by 38%. It is obvious from Table 1 that $\bar{n}$ changes in the reverse direction of $[M]_p$. We cannot decouple $[M]_p$ from $\bar{n}$. It is reasonable to assume that $[M]_p$ increases with stirring speed so as a result $\bar{n}$ should decrease. However, the drop in $\bar{n}$ is seemingly more significant than the rise in $[M]_p$. It can be concluded that increasing S_r, as well as increasing rpm, improves the rate of monomer transport from the droplets to the particles until it approaches the rate of polymerisation under saturated conditions; reaction controlled. Particles are most likely saturated with MMA monomer at $S_r = 500\%$ because R_p does not further decrease with increasing S_r beyond this point (not shown). Arai et al. [8] also provided a strong evidence for monomer-transport limitation in the emulsifier-free emulsion polymerisation of MMA carried out under the conditions similar to those used in this research.

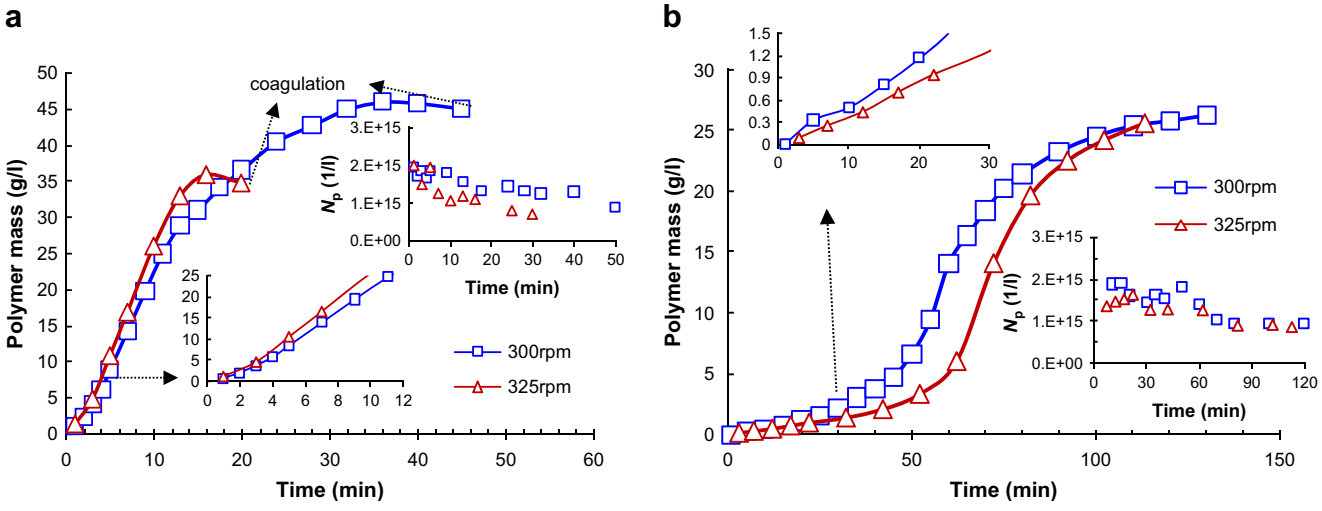

Fig. 9. Polymer mass versus time at two rpm for (a) MA, and (b) MMA monomers. The insets in figures (a) and (b) show the early polymer mass–time and N_p–time data, respectively ($S_r = 150\%$ and 200% for MA and MMA monomers, respectively).

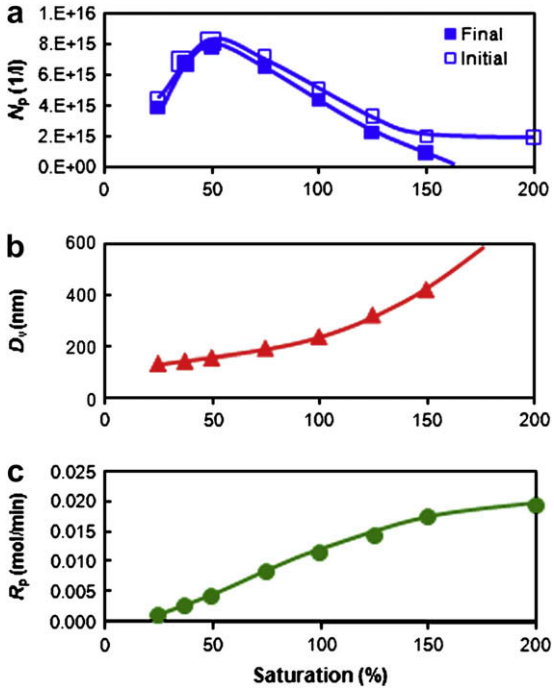

Fig. 10. The variations in (a) N_p, (b) final D_v, and (c) R_p with monomer saturation ratio for MA polymerisation (note that R_p in Figs. 10–12 is based on the number of moles of monomer reacted in 600 ml of water).

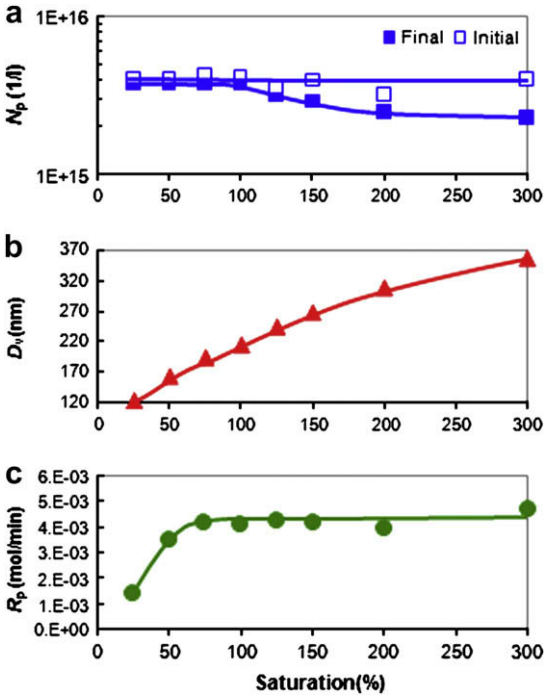

Fig. 11. The variations in (a) N_p, (b) final D_v, and (c) R_p with monomer saturation ratio for VA polymerisation.

4.3. Particle formation

The time evolution of the number of particles demonstrates most clearly the effect of monomer concentration on the particle formation and coagulation. Obviously we could not monitor coagulation of primary particles during nucleation stage due to its fast dynamics; however, the degree of particle coagulation during the growth stage was monitored and is judged by the number of particles lost in the course of polymerisation.

Fig. 10 shows the final and initial N_p, final D_v, and R_p for MA monomer. The values for the initial (maximum) number of primary particles were extracted from the size data in the early minutes of reactions. It is quite likely that the real maximum in the number of particles could have occurred at an earlier time [19]. We think, however, that the first maximum measured is useful for this discussion as it can represent the extent of particle coagulation in the course of polymerisation. The average size of particles increased almost exponentially with MA concentration. The number of particles was maximum when monomer saturation ratio was 50%. This may not be an artefact as the whole curve was reproduced. It is clear from Fig. 10 that particle coagulation during the growth stage is negligible at $S_r \leq 50\%$, but becomes progressively more important at higher S_r ratios (note that the coagulation of precursor particles is beyond this discussion). The rate of polymerisation continues to increase with monomer concentration for $S_r > 100\%$, but at a low rate, indicating a declining diffusion-controlled monomer transport.

Fig. 11 shows the initial and final N_p, final D_v, and R_p for VA monomer. Almost the same number of particles was initially formed for the range of monomer concentrations used in this study. The final N_p remained almost constant for $S_r \leq 100\%$ as particle coagulation practically did not occur within this range of monomer concentration. A constant number of particles in the range of $S_r \leq 100\%$ is in contrast with the data of Dunn and Taylor [20] who reported a decreasing number of particles with increasing S_r in the same region, but is in accordance with the data reported by Napper and Parts [21] indicating a constant N_p in the range of $67\% < S_r < 100\%$ (0.22–0.33 mol/l). The rate of coagulation, however, increased with monomer saturation ratio for $S_r > 100\%$ resulting in a gradual decrease in N_p. This could be possibly the reason for a slight decrease in the rate of polymerisation in the intermediate range of conversion with increasing S_r.

Fig. 12 depicts the initial and final N_p, final D_v, and R_p for MMA monomer. The size of final particles increased significantly with monomer concentration for $S_r < 100\%$, reached a maximum at $S_r = 100\%$ and then decreased slightly for $S_r > 100\%$ (Fig. 12b). The results indicate that the number of initial particles was almost constant for $S_r \leq 100\%$. Particle coagulation was negligible at $S_r = 25\%$ but became increasingly more significant with monomer concentration up to $S_r = 100\%$. The rise in the rate of coagulation with monomer concentration in this region is associated with a rise in R_p. Particle coagulation continuously declined with increasing monomer concentration for $S_r > 100\%$ due to concomitant decrease in R_p, until it almost ceased to exist for $S_r = 500\%$. As a result of these opposing trends, a minimum in N_p appeared in the region of $S_r = 100\%$. Using a mathematical model, Arai et al. [8] predicted that the number of particles in emulsifier-free emulsion polymerisation of MMA continuously increases with monomer concentration until the saturation concentration is reached. An opposite trend was produced in this research.

The mechanistic understanding of particle nucleation in emulsion polymerisation has immensely improved over the last two decades. However, the integration of particle coagulation with particle formation is still the weakest link of the nucleation models. The major difficulty with inclusion of coagulation is that the treatment contains many parameters whose values are difficult to determine, as well as making it difficult to judge the correctness of the model assumptions [11]. This, together with diffusion-controlled monomer transport occurring in the starved systems persuades us to adopt a qualitative approach in order to explain the wide disparity in the particle numbers. The rate of particle formation via homogeneous nucleation mechanism is:

$$\frac{dN_p}{dt} = R_{gen} - R_{coag} \tag{12}$$

where R_{gen} is the rate of precursor particle formation given as:

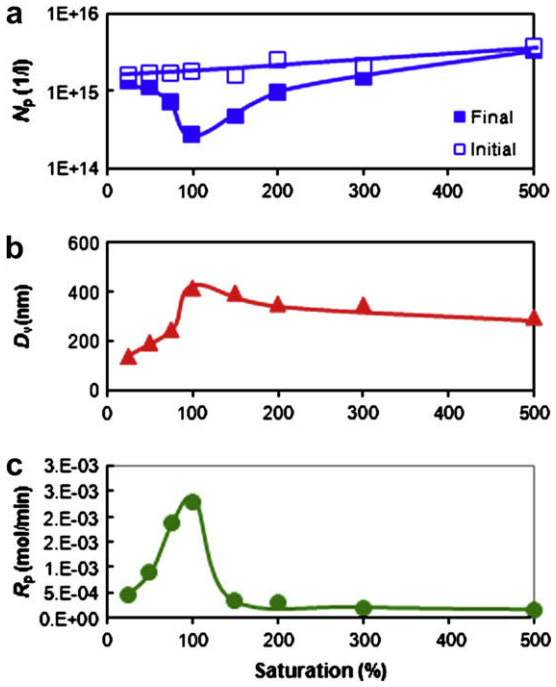

Fig. 12. The variations in (a) N_p, (b) final D_v, and (c) R_p with monomer saturation ratio for MMA polymerisation.

$$R_{gen} = k_{pw}^{j_{cr}-1}\left[IM_{j_{cr}-1}^{\circ}\right][M]_w \tag{13}$$

where $k_{pw}^{j_{cr}-1}$ is the propagation rate constant for a growing radical with the chain length of $j_{cr}-1$ and $[IM_{j_{cr}-1}^{\circ}]$ is the concentration of the initiator-derived radical in the water phase given as [11]:

$$\left[IM_{j_{cr}-1}^{\circ}\right] = \frac{k_{pw}^{j_{cr}-2}\left[IM_{j_{cr}-2}^{\circ}\right][M]_w}{k_{pw}^{j_{cr}-1}[M]_w + k_{tw}[R^{\circ}] + k_{ap}^{j_{cr}-1}N_p} \tag{14}$$

where $[R^{\circ}]$ is the total radical concentration $(=\sum_{i=1}^{j_{cr}-1}[IM_i^{\circ}])$, k_{ap} is the rate constant of the capture of radicals by polymer particles. The capture rate constant is given by Smoluchowski as:

$$k_{ap}^{j_{cr}-1} = 4\pi D_{j_{cr}-1} r_p N_A \tag{15}$$

where r_p is the swollen particle diameter and $D_{j_{cr}-1}$ is the diffusion coefficient of a radical with chain length $j_{cr}-1$ in the water phase. It can be inferred from Eqs. (13)–(15) that the rate of particle formation is significantly affected by $[M]_w$.

R_{coag} is the rate of particle coagulation which can be shown by:

$$R_{coag} = kN_p^2 \tag{16}$$

where k is a complicated function of particle size and charge density. The rate of particle coagulation is purely electrostatic and function of surface charge density on the particles, given the ionic strength of the aqueous medium is constant in the system under study. This charge is theoretically composed of the ionic end groups and *in situ* generated surfactants. For monomers with a high water solubility and propagation constant, such as those studied in this work, the formation of *in situ* surfactants in the water phase appears to be negligible. Whichever the source is, R_{coag} is expected to increase with the size of primary particles with a fixed number of ionic end groups attached. Particles that undergo fast polymerisation are more vulnerable to particle coagulation because of their large size and small surface charge density. A fast rate of polymerisation could simply be due to a large k_p (as is the case for MA monomer), a high $[M]_p$ (as is the case for monomer-swollen particles during polymerisation), or a large $\bar{n}$ (as is the case for termination-controlled polymerisation of MMA monomer under starved conditions).

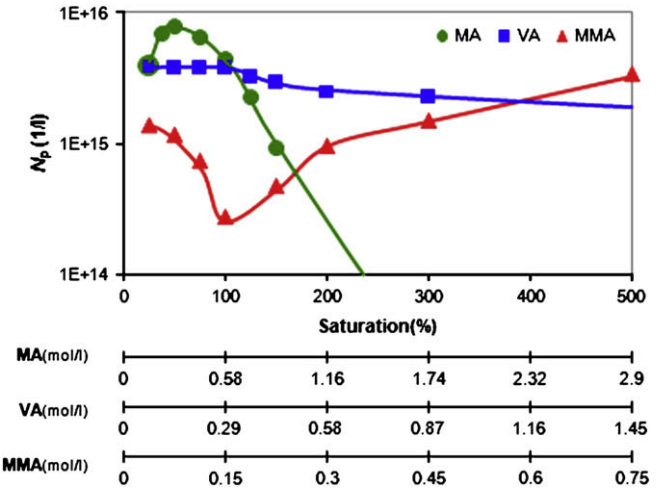

Fig. 13. N_p versus monomer saturation ratio for MA, VA, and MMA polymerisations (the second abscissa is in terms of molar concentration of corresponding monomers).

There are at least two competing effects in the starved region ($S_r \leq 100\%$). A lower concentration of monomer in the water phase decreases the rate of radical propagation in the water phase and as a result the rate of particle formation (note that the rate of initiator decomposition may be also altered by a change in the monomer concentration in the aqueous phase leading to further reduction in the rate of radical generation). Counteracting this is that particles usually grow at a reduced rate under monomer-starved conditions (except for PMMA particles) and as a result they are more stable (for a fixed number of attached initiator-derived radicals) and thus less vulnerable to particle coagulation. Therefore, both particle formation and coagulation are usually depressed under starved conditions. The number of particles in terms of S_r is thus determined by the extent to which these reductions occur. This may dictate different trends for different monomers such as the occurrence of the minimum in N_p for MMA monomer and the maximum for MA monomer.

In the monomer-saturated range ($S_r \geq 100\%$), where the water phase is saturated with monomer, the number of particles is dictated by the rate of particle growth/coagulation as the rate of particle formation is expected to remain constant. The comparison of the final number of particles with the initial number of particles indicates a significant coagulation occurred during the nucleation and growth stages. The decrease in the number of particles with reaction time is one of the common features of emulsifier-free emulsion polymerisations [3,22]. A high rate of propagation for MA monomer, that allows a rapid growth for the particles, plays the main role for the extensive coagulation during this polymerisation. Particle coagulation occurred to an intermediate degree for VA monomer. For MMA monomer, the rate of particle coagulation progressively decreased with increasing S_r because of a concomitant drop in R_p, as explained before.

One may expect that the rate of particle coagulation to be also affected by the state of polymer particles. The glass transition temperature of polymethyl acrylate, polyvinyl acetate and polymethyl methacrylate is approximately −30 °C, 28 °C, and 104 °C, respectively. Polymethyl methacrylate is therefore the hardest latex among three at the reaction temperature of 60 °C. Nevertheless, results show significant particle coagulation for this monomer.

Fig. 13 compares the final number of particles obtained for the monomers in terms of S_r as well as concentration of individual monomers (mol/l). At a low S_r, where the effect of particle

coagulation was minimum for some monomers, the number of particles produced was in the order of water solubility of monomers; MA > VA > MMA. This pattern changed significantly with increasing monomer concentration as particle coagulation became progressively more important for some monomers. At $S_r = 500\%$, the order was reversed so that the largest number of particles was obtained for the least water-soluble monomer studied; MMA.

5. Conclusions

The monomer concentration strongly affects the number of particles formed in emulsifier-free emulsion polymerisations depending on monomer type and solubility. The results indicate that particle formation via homogeneous nucleation is a complex function of monomer concentration in the water phase, concentration of monomer droplets, and the rate of polymerisation. There are two distinctive regions in terms of monomer concentration:

1- Monomer-starved region ($S_r < 100\%$): the rate of polymerisations increases with monomer concentration almost for all monomers. For MA monomer, the maximum number of particles was obtained at monomer saturation ratio of 50%. Emulsion polymerisations of VA showed almost no variation in the number of particles in this region. For MMA, the number of particles decreased significantly with increasing S_r due to significant rate of particle coagulation.

2- Monomer-saturated region ($S_r > 100\%$): the rate of polymerisation increased with monomer concentration for MA monomer, remained constant for VA monomer and decreased for MMA monomer. Particle coagulation occurred moderately in the course of polymerisation for VA monomer but severely for MA monomer. The extent of particle coagulation for MMA monomer decreased with increasing monomer concentration. The maximum rate of coagulation for MMA corresponds to the maximum rate of polymerisation that occurred when the water phase was saturated with the monomer; $S_r = 100\%$. Evidence was found that particles may not be saturated with monomer when S_r is not significantly greater than 100%.

References

[1] Goodwin JW, Hearn J, Ho CC, Ottewill RH. Colloid and Polymer Science 1974;252(6):464–71.
[2] Fitch RM, Prenosil B, Sprick KJ. Journal of Polymer Science, Part C: Polymer Symposium 1969;27PC:95–118.
[3] Fitch RM. British Polymer Journal 1973;5:467–83.
[4] Hansen FK, Ugelstad J. Journal of Polymer Science, Part A: Polymer Chemistry 1978;16:1953–79.
[5] Feeny PJ, Napper DH, Gilbert RG. Macromolecules 1987;20:2922–30.
[6] Goodwin JW, Hearn J, Ho CC, Ottewill RH. British Polymer Journal 1973;5:347–62.
[7] Tanrisever T, Okay O, Sonmezoglu IC. Journal of Applied Polymer Science 1996;61:485–93.
[8] Arai K, Arai M, Iwasaki S, Saito S. Journal of Polymer Science, Part A: Polymer Chemistry 1981;19:1203–15.
[9] Chern CS, Lin CH. Polymer Journal 1995;27:1094–103.
[10] Sajjadi S, Brooks BW. Journal of Applied Polymer Science 1999;74:3094–110.
[11] Gilbert RG. Emulsion polymerisation: a mechanistic approach. London: Academic Press; 1995.
[12] Trommsdorff E, Kohle H, Lagally P. Macromolecular Chemistry and Physics 1948;1(3):169–98.
[13] Brooks BW, Wang J. Polymer 1993;34:119–23.
[14] Sajjadi S. Langmuir 2007;23:1018–24.
[15] Zimmt WS. Journal of Applied Polymer Science 1959;1:323.
[16] Ballard MJ, Napper DH, Gilbert RG. Journal of Polymer Science, Part A: Polymer Chemistry 1984;22(11):3225–53.
[17] Nomura M, Fujita K. Polymer Reaction Engineering 1994;2:317–45.
[18] Nomura M. In: Piirma I, editor. Emulsion polymerisation. Academic Press; 1982. p. 191.
[19] Kuhn I, Tauer K. Macromolecules 1995;28:8122–8.
[20] Dunn AS, Taylor PA. Macromolecular Chemie 1965;83(APR):207–19.
[21] Napper DH, Parts AG. Journal of Polymer Science 1962;61:113–26.
[22] Goodall AR, Wilkinson MC, Hearn J. Journal of Polymer Science, Part A: Polymer Chemistry 1977;15:2193–218.